January 2012

Alterations In Regional Cerebral Blood Flow With Propofol Anesthesia Compared With Sevoflurane

Tejas Manchandia

ALTERATIONS IN REGIONAL CEREBRAL BLOOD FLOW WITH PROPOFOL ANESTHESIA COMPARED WITH SEVOFLURANE

A Thesis Submitted to the
Yale University School of Medicine
in Partial Fulfillment of the Requirements for the
Degree of Doctor of Medicine

by

Tejas Chandrakant Manchandia

2012

ABSTRACT

ALTERATIONS IN REGIONAL CEREBRAL BLOOD FLOW WITH PROPOFOL ANESTHESIA COMPARED WITH SEVOFLURANE. Tejas Manchandia, Maolin Qiu, Margaret Rose, Todd Constable, and Ramachandran Ramani. Department of Anesthesiology and Department of Diagnostic Radiology, Yale University School of Medicine, New Haven, CT.

Alterations in regional cerebral blood flow (rCBF) are a reflection of neuronal activity in the brain because of the property of flow-metabolism coupling. Our group has previously reported a non-uniformity in rCBF changes with 0.25 MAC sevoflurane. The purpose of this project was to measure the alteration in rCBF with 0.5 MAC equivalent propofol and compare the changes in rCBF with those observed previously with sevoflurane. We hypothesize that sevoflurane and propofol produce spatially non-uniform changes in rCBF, with significant decreases in the thalamus and prefrontal cortex. The study protocol was approved by the Yale University Human Investigation Committee (HIC). The subjects were 30 healthy volunteers (19-35 years old). Propofol was administered through a target controlled infusion (TCI) device to a target plasma concentration of 2 μg/mL (0.5 MAC equivalent). Propofol level was confirmed by drawing a blood sample at the beginning and end of the infusion period. Regional CBF was measured in a 3 Tesla Siemens Trio scanner using the pulsed arterial spin labeling (PASL) technique. CBF was measured in the subjects while awake and under anesthesia, and the difference was calculated (δCBF). With 2 μg/mL plasma level propofol, there was a drop in rCBF in several areas of the frontal, parietal, occipital, and temporal cortices as well as the

thalamus. Clinically, all the subjects were asleep and had no memory of the event. A modest rise in rCBF was seen in the anterior cingulate, insula, and parahippocampal gyrus. Our results support our hypothesis that propofol causes a non-uniformity in rCBF, which was observed with sevoflurane as well.

ACKNOWLEDGEMENTS

This research project was made possible by funding from the Yale Office of Student Research at Yale University School of Medicine.

Thanks to Dr. Todd Constable his support of medical student research at Yale and his effort to inspire an appreciation of functional magnetic resonance imaging. Thanks to Maolin Qiu for conducting the data analysis. Special thanks to Dr. Ramachandran Ramani for his many hours of guidance and support both through the research process and the completion of this manuscript.

Finally, thank you to my family and friends for their love and support through all of my endeavors.

TABLE OF CONTENTS

INTRODUCTION

Although general anesthetic agents have been used extensively for over 160 years, their mechanism of action on brain physiology remains poorly understood. The two main classes of general anesthetics are intravenous agents, such as propofol, and volatile agents, such as sevoflurane [1]. The primary goal in anesthesia is to induce amnesia, analgesia, hypnosis, muscle relaxation, and suppression of reflex motor response.

Propofol, one of the most commonly used anesthetic agents, is a potent short-acting intravenous agent used for induction and maintenance of general anesthesia [2]. Despite being used widely for over 20 years, its exact functional target and neural mechanism remains unknown. There have been several proposed mechanisms of action of propofol-induced anesthesia, including potentiation of γ-aminobutyric acid (GABA) receptor activity and acting as a sodium channel blocker [3, 4, 5]. Studies have also shown that propofol interacts with and influences the release of various other neurotransmitters, including glycine, acetylcholine, glutamate, and serotonin, with concentrations varying in different regions of the brain following propofol-induced anesthesia [6, 7]. However, the most accepted theory is that propofol produces its effects by positive modulation of the agonist effects of GABA at the $GABA_A$ receptor level, as opposed to effects occurring at the axonal pathway [6, 8, 9].

In contrast, sevoflurane is an inhaled agent used for induction and maintenance of general anesthesia with a rapid onset and offset of action. It acts on many areas in the CNS, but its precise mechanism of action also remains unknown. Some areas that play a role in consciousness and are likely suppressed by sevoflurane and other inhaled anesthetic agents include the cerebral cortex, thalamus, limbic system and reticular

formation [10]. In terms of its mechanism of action, it is widely believed that sevoflurane potentiates inhibitory postsynaptic channel activity at $GABA_A$ and glycine receptors, as well as inhibits excitatory postsynaptic channel activity at nicotinic acetylcholine, serotonin, and glutamate receptors [8]. However, there is no definitive evidence as to its exact targets in the brain or its neural mechanism.

Recent advancements within the field of brain imaging offers great potential to better understand the mechanism of these anesthetic agents [11]. The two most common and most powerful imaging techniques used to study human brain activation are positron emission tomography (PET) and functional magnetic resonance imaging (fMRI), which are both capable of mapping regional changes in cerebral blood flow that occur as a result of alterations in brain activity, with increased blood flow in areas where neuronal activity increases [10, 11, 12]. PET is also able to measure changes in metabolism, while fMRI is able to measure changes in blood oxygen level dependent (BOLD) signal (a qualitative measure of neuronal activity). In contrast to prior studies looking at changes in neuronal activity as recorded by electroencephalogram (EEG), PET and fMRI can objectively measure the subjective behavioral responses associated with anesthesia [1, 11].

PET Imaging

In a PET scan, cerebral metabolic rate of glucose consumption (CMRGlu) is measured with [^{18}F]fluorodeoxyglucose (^{18}FDG), and regional cerebral blood flow (rCBF) is measured with ^{15}O-labeled water ($H_2{}^{15}O$) [13]. PET studies allow for measurements of neuronal activity by measuring the changes in CBF or CMRGlu induced by neuronal activity. In studying the effects of anesthetic agents, earlier studies

conducted using PET have shown a global decrease in metabolic activity reflecting the reduced neuronal activity in the brain under anesthesia [14, 15, 16]. However, subsequent PET studies have not only shown a generalized decreased in activity in the brain, but have also revealed regional variations in the amount of reduction in activity, especially with inhaled anesthetic agents [10, 17, 18]. The differences were most drastic when comparing volatile agents with propofol, which is consistent with the suggested notion that propofol has a different mechanism of action than inhaled agents, such as sevoflurane [19, 20].

Specifically, PET studies looking at the effects of isoflurane on human cerebral glucose metabolism have shown a nearly uniform reduction in whole-brain metabolic activity [15]. Similarly, studies looking at the effects of the inhaled anesthetic agent halothane on human cerebral glucose metabolism have shown whole-brain metabolic reduction with significantly less relative metabolism in the basal forebrain, thalamus, limbic system, cerebellum, and occiput while under high dose anesthesia [11, 16].

Propofol too has been shown to induce a dose-dependent decrease in cerebral blood flow [21, 22, 23, 24]. When looking at cerebral metabolism during propofol anesthesia with PET, cortical metabolism decreased in all areas under anesthesia, but was not uniform [14, 23]. In contrast to inhaled anesthetics, cortical metabolism was more significantly depressed in comparison to subcortical metabolism, and the largest percent decrease was found to occur in the left anterior cingulate and the inferior colliculus [14, 19, 20]. In addition, when looking at rCBF, large regional decreases have been shown to occur bilaterally in the medial thalamus, the cuneus and precuneus, and the posterior cingulate, orbitofrontal, and right angular gyri [23]. However, it is important to note that

these studies found non-uniform changes in rCBF, with some areas having a decrease in rCBF and others having an increase, though there could be overlapping regions obscuring other findings [10, 17, 18].

Although PET studies have revealed parts of the neuroanatomical regions important for anesthetic action, they have a low intrinsic spatial and temporal resolution [25]. They are based on a measurement at one point in time, and multiple measurements are difficult due to the half-life of the isotopes used. In addition, PET studies require the injection of isotopes, and multiple blood samples must be drawn during the study. In contrast, fMRI provides higher temporal and spatial resolution, does not necessitate the use of an exogenous tracer, and does not require a blood draw, allowing for multiple measurements in a single study [25].

MRI—Basic Principles

In a conventional MRI scan, a strong external magnetic field is used to align the H^+ spins with the direction of the field. A radiofrequency (RF) pulse is then used to produce a varying electromagnetic field. The RF pulse has the correct resonance frequency to flip the spin of all the protons, and when it is turned off, the spins begin to return to their thermodynamic equilibrium [26]. The receiving coils then measure the radiofrequency signal generated by these protons returning to equilibrium. This radiofrequency signal is structure specific, allowing for the structural image to be mapped based on the signal generated. By applying different magnetic field gradients, images can be obtained in different orientations.

Functional MRI (fMRI)

In contrast to conventional MRI, which produces static structural images, fMRI is used to detect changes in the brain caused by neuronal activity. BOLD and rCBF are the two measures of neuronal activity measured in fMRI.

Blood Oxygen Level Dependent (BOLD) Contrast

BOLD is based on the concept that there are differences in magnetic properties between arterial and venous blood due to differences in oxygen concentration, forming the basis for blood oxygen level dependent (BOLD) intrinsic contrast. Specifically, deoxyhemoglobin has paramagnetic properties and oxyhemoglobin does not, and BOLD is sensitive to local changes in deoxyhemoglobin concentration [26]. The BOLD signal is proportional to the ratio of oxyhemoglobin to deoxyhemoglobin. With increased neuronal activity, there is an increase in oxygen consumption as well as cerebral blood flow. However, the increase in blood flow is out of proportion to the increase in metabolism and oxygen consumption, resulting in a lower concentration of deoxyhemoglobin in areas of increased activity, which forms the basis of BOLD [27, 28]. Thus, with increased neuronal activity and less deoxyhemoglobin as a result of a greater increase in regional cerebral blood flow, there would be less spin dephasing and an increase in MR signal [27]. It is important to note that BOLD is a qualitative measure of neuronal activity; hence, the relative change in BOLD is more important than the absolute BOLD value.

Pulsed Arterial Spin Labeling (PASL) Technique

For measuring rCBF, perfusion imaging is done by differentiating the arterial water proton spins from the tissue water spins using a labeling technique, such as arterial spin labeling (ASL), and then observing the signal change following the free diffusion of the arterial water with tissue water [29, 30]. The common principles of perfusion imaging is that the concentration of a tracer must be known within the arterial blood supply and in the tissue, as well the partition coefficient of the tracer [31]. In ASL, this occurs through proximal labeling of arterial water spins using a selective preparation sequence, and acquiring two successive images after a small delay of time. Subtraction of these images, one with and one without the labeling of the freely diffusible arterial water, allows us to calculate the perfusion to a certain region of the brain [32]. In contrast to BOLD intrinsic contrast, which is heavily weighted toward venous outflow, arterial spin labeling is a measurement at the capillary level, making it a relatively more accurate assessment of neuronal activity [33]. Moreover, the absolute rCBF is measured in pulsed arterial spin labeling (PASL).

In the PASL technique, a short radiofrequency (RF) pulse is used to invert the longitudinal magnetization spin of the arterial blood upstream of the region of interest (ROI), as described in Figure 1. Using spin echo imaging, the difference in signal between measurements with and without labeling allows for calculation of the amount of blood arriving to that particular volume of the brain. Because the labeling is done closer to the acquisition plane, there is a much better signal-to-noise ratio with PASL [32]. Prior to the advent of PASL, one major problem in perfusion imaging was the variable arterial transit time from the labeling to the region of interest, during which longitudinal

relaxation of the labeled spin led to a decrease in signal [30]. However, due to the drastically reduced transit time with PASL, it is possible to get a much more accurate quantification of cerebral blood flow to a particular region of interest [30]. Nonetheless, the rapid imaging required in PASL does reduce the spatial resolution to an extent.

Figure 1. Illustration of pulsed arterial spin labeling. White circles with down arrows represent the magnetized spins (protons). Gray circles with upward arrows represent those spins that have flipped back as they pass through the capillary bed. The proportion is a direct measurement of perfusion. Adapted from Golay X et al. 2004, ©Lippincott Williams & Wilkins [32].

Due to the property of neurovascular coupling in the brain, changes in blood flow accurately reflect changes in neuronal activity. Neurovascular coupling was first described in 1890, and refers to a range of mechanisms that exist in the brain that work on arteriolar tone to adjust blood flow according to metabolic needs [34, 35, 36]. This

allows CBF to be an accurate representation of the change in cerebral metabolic rate of oxygen ($CMRO_2$). However, studies have shown that pathological conditions that disrupt capillary morphology, including amyloid, diabetes, or hypertensive microangiopathy, may result in inaccurate flow-metabolism coupling [35]. Hence, flow-metabolism coupling is best used as a measure of neuronal activity in healthy subjects.

Anesthesia and fMRI

Despite the great potential of fMRI to study the effects of anesthetic agents on the brain, only a small number of studies have been done. Functional MRI studies done using subanesthetic concentrations of volatile agents have shown a decrease in activity in specific neural networks with decrease in activation induced response rather than a global decrease in neuronal activity [25, 33]. Specifically, Heinke et al. (2001) used subanesthetic doses of isoflurane in healthy volunteers to study task-induced brain activation. Activation induced response allows one to study specific areas of the brain by using tasks known to activate that area and measure changes in activity at baseline and with an anesthetic to determine the change in activity caused by the anesthetic agent. Heinke et al. (2001) found that isoflurane caused a decrease in visual search task-induced brain activation in the right anteriosuperior insula and the banks of the left and right intraparietal sulcus, but no change in areas associated with primary information processing, including the lateral geniculate nucleus, primary visual cortex, and motor cortex [25]. Similarly, 0.25 MAC sevoflurane has been shown to decrease task-induced activation in the primary and secondary visual cortices, thalamus, hippocampus, and supplementary motor area without causing a significant global decrease in activity [33].

These fMRI studies have reported a relatively greater spatial resolution then previously seen with PET imaging [23, 27].

Our prior studies have shown 0.5 MAC sevoflurane to decrease rCBF in various areas of the frontal, parietal, temporal, and occipital lobes, as well as in the anterior cingulate, cingulate gyrus, lentiform nucleus, thalamus, and cerebellum. In addition, we found sevoflurane to cause an increase in rCBF in the superior temporal gyrus, middle temporal gyrus, lingual gyrus, parahippocampal gyrus, anterior cingulate, cingulate gyrus, claustrum, insula, and pons. In the present study, we are investigating the influence of 0.5 MAC equivalent propofol anesthesia on rCBF in healthy volunteers in order to better understand the mechanism of action of propofol and compare it to the equivalent dose of sevoflurane.

STATEMENT OF PURPOSE

The goal of this study is to help us better understand how two commonly used anesthetic agents (propofol and sevoflurane) affect the central nervous system and the similarities and differences in their effects. This in turn will help in selecting the appropriate combination of anesthetic drugs in patients, with minimal side effects. These experiments also give us information on how the central nervous system communicates form cortical to subcortical areas. Moreover, given the recent concern regarding the neurotoxic effects of anesthetic agents, this study will allow us to better understand which areas of the brain are most affected by two commonly used anesthetic agents. These areas can then further be studied in animal models to determine if general anesthetics do in fact have neurotoxic effects leading to neurodegeneration. We hypothesize that "sevoflurane and propofol produce spatially non-uniform changes in rCBF, with some areas manifesting a decrease in rCBF and others an increase." This study will also clarify the similarities and differences between the two commonly used anesthetic agents at clinically relevant concentrations.

METHODS

The study protocol was approved by the Yale University Human Investigation Committee.

Subjects

Thirty consenting American Society of Anesthesiologists (ASA) patient classification status I healthy volunteers aged 19 to 30 years old were studied. All subjects were required to go through a clinical screening, including a history and physical examination, within 7 days prior to the study. Screening involved a history of any medical problems, surgical history, medication use and any history of adverse reactions to anesthesia. The physical exam involved checking vitals signs (heart rate, blood pressure, respiratory rate), auscultation to rule out cardiac and respiratory problems, and an airway exam to ensure that the subject was not prone to airway obstruction during anesthesia. Only ASA class I subjects with no systemic problems and body weight within 20% of the ideal weight for their height were selected for the study.

Exclusion criteria:

1) Subjects with a history of milk or egg allergy were not included.

2) Subjects on centrally acting medications such as antidepressants were not included.

3) Those subjects with contraindications to MRI (e.g. subjects with metal implants) were also excluded.

The experimental protocol of imaging and anesthesia were described to all subjects before the study. All subjects completed a MR safety questionnaire. Subjects were given a consent form to take home, read, and have ample time to seek any

clarifications. On the day of the study, they brought the signed consent form and had any remaining questions answered. On arrival at the Magnetic Resonance Research Center, the subjects were screened for the presence of any ferromagnetic substance and other contraindications for MRI. Subjects were checked with a metal detector prior to entering the MR scan room. Female subjects were required to undergo a urine pregnancy test, and only those subjects having a negative pregnancy test were included in this study. Although no harmful biological effects of MRI on pregnancy have been identified to date, it is the policy of the Yale HIC to exclude pregnant women in all MRI research studies. All subjects were weighed prior to the study and an intravenous (IV) cannula was placed under sterile conditions for Propofol infusion. A second IV cannula was placed under sterile conditions for drawing blood samples for propofol assay, which is described below. Subjects were monitored as per ASA basic standards of monitoring. Sedation level was evaluated and graded according to the observer's assessment of alertness/sedation (OAA/S) rating scale (Figure 2).

Figure 2. Observer's assessment of alertness/sedation (OAA/S). Adapted from Clouzeau et al. 2010 [37, 38].

Anesthesia

All subjects were told to fast for eight hours prior to the study. Propofol anesthesia was administered through a Target Controlled Infusion (TCI) device (STANPUMP pump connected to a Harvard 22 syringe pump). STANPUMP is available from Steven L. Shafer, M.D., Anesthesiology Service (112A), PAVAMC, 3801 Miranda Ave., Palo Alto, CA 94304. STANPUMP is a pharmacokinetic infusion program (also referred to as the target controlled infusion—TCI pump). This software in a laptop drove the Harvard 22 syringe pump at the required rate (depending on the subject's pharmacokinetics) in order to achieve the selected target propofol level. The selected TCI propofol plasma level was 2 μg/mL (equivalent to 0.5 MAC level), with the rate of infusion determined by the subject's weight, height, and sex. For anesthesia, the required propofol plasma level is 3-4 μg/mL. Subjects inhaled oxygen through a nasal cannula at 4 liters per minute throughout the study. An experienced anesthesiologist was present throughout the entire assessment, and full anesthesia and resuscitation equipment was always available. Propofol level was confirmed by drawing a 3 cc blood sample at the beginning and end of the propofol infusion period. Blood samples were stored at -80°C and sent to a UCSF laboratory for propofol assay.

Imaging

Magnetic resonance imaging data were acquired on a 3 Tesla whole-body scanner Trio (Siemens Medical Systems, Erlangen, Germany) with a 12-channel phased-array head coil. Pulsed arterial spin labeling imaging was used to measure perfusion-induced changes in image signal intensity during the resting state. The QUIPSS PASL sequence

was used for measuring the resting-state CBF in the awake and anesthesia conditions [39]. Interleaved labeling and control images were acquired using a gradient echo-planar imaging (EPI) sequence. A slab-selective (100 mm) hyper-secant inversion radiofrequency (RF) pulse was used for ASL. The RF pulse was applied to a slab 25 mm inferior to the imaging slab and the same RF pulse was applied to a slab 25 mm superior to the imaging slab to control the off-resonance effects. A 20-slice ASL acquisition was implemented and all slices were AC-PC angled and positioned to fully cover the brain cortex. The ASL acquisition parameters were: field of view FOV = 256×256 mm^2; matrix = 64×64; bandwidth = 2004 Hz/pixel; slice thickness = 5 mm, and inter-slice gap = 2.5 mm. The repetition time was TR = 3000 ms; the echo time was TE = 26 ms. Acquisition of each slice took approximately 60 ms, therefore the post-labeling inversion time for each slice i, i = 1, 2, …, TI(i) = $1400+60 \times (i-1)$ ms, which was used in CBF quantification, resulting a data acquisition window of 1.4 to 2.6 seconds after labeling. Proton density weighted images were collected using the same perfusion sequence, except for the following changes: TR was set to 10 seconds; the delay time TD was set to 0 ms; and the inversion time TI was set to maximum. Two additional acquisitions were acquired to aid in multi-subject registration. First, a high-resolution whole brain 3D structure image was acquired for each subject using MPRAGE (Magnetization Prepared Rapid Acquisition with Gradient-Echo imaging), with the following settings: 160 sagittal slices with FOV = 256×256 mm^2; voxel size = $1 \times 1 \times 1$ mm^3; TR = 1500 ms; TI = 800 ms; TE = 2.83 ms; flip angle 15 degrees; and one average. Next, two sets of multi-slice 2D T_1-weighted images, each for one part of the brain, were acquired during each MR session using the same slice positions as the perfusion-weighted images with the

following settings: FOV = 256×256 mm^2; in-plane resolution 1×1 mm^2; TR = 300 ms; TE = 3.69 ms; flip angle 60 degrees; and two averages.

The subjects stayed still with eyes closed in the scanner during the MRI experiment. Two PASL runs, each of 200 volumes, were acquired for the awake condition and for the anesthesia conditions, respectively. For the anesthesia condition, the MRI scans only started ~10 minutes after the anesthetic was delivered to the subjects. These perfusion-weighted data were later used to calculate absolute CBF on a per-voxel basis.

Quantification of Regional Cerebral Blood Flow

Perfusion-weighted and the proton-density weighted images were motion-corrected using the Statistical Parametric Mapping package (SPM99), via a 6-parameter rigid-body transformation. Time series of the perfusion-weighted images were obtained by pair-wise "surround" subtraction between interleaved label and control pairs for either the resting state, resulting in a temporal resolution of 2TR [40, 41, 42]. Perfusion-induced difference maps (ΔM) were calculated by averaging all the difference images in the time series for the whole resting state. The mean image of the motion-corrected proton density images (M_0) was estimated by averaging multiple acquisitions. The absolute CBF (f) (ml/100g/minute) was calculated:

$$\Delta M(t) = M^{ctrl}(t) - M^{label}(t) = \frac{2cf(t-\tau_a)M_0^*}{\lambda} e^{-t/T_{1a}} \qquad (1)$$

in which,

λ is the tissue-blood partition coefficient for water;

$$c = \alpha_{\pi} \frac{1 - e^{-(t-\tau_a)(1/T_{1app} - 1/T_{1a})}}{(t-\tau_a)(1/T_{1app} - 1/T_{1a})} \quad (2)$$

is the correction factor, which accounts for exchange of labeled magnetization from intravascular to extravascular space and clearance of the labeled blood water out of the capillary bed;

τ_a is the arterial transit time, which is the time for the labeled blood water to arrive at the capillary bed after labeling, and

$$M_0^* = M_0 e^{-TE/T_2^*}. \quad (3)$$

T_{1app} is the apparent longitudinal relaxation time. In Equation (2), when $(t-\tau_a)(1/T_{1app} - 1/T_{1a})$ is small, $c \approx \alpha_{\pi}$. Other parameters used in CBF quantification: $T_{1a} = 1490ms$, $\lambda = 0.9ml/g$, $\alpha_{\pi} = 0.95$, $t - \tau_a = 700ms$, and $TI = 1400\ ms$ for the first slice. After M_0^*, T_{1app}, and ΔM have been measured on a per-voxel basis, CBF (*f*) can then be estimated using Equation (1).

Inter-Subject Data Integration

A standard whole brain template (MNI-1mm) was used for subject spatial normalization of the group data. Registration of multiple subject data and group analyses were carried out using the BioimageSuite software package bioimagesuite.org [43]. Two transformations were performed to allow multiple subject integration: first, a linear

transformation was estimated by co-registering the subject's multi-slice 2D T_1-weighted images to the high-resolution 3D anatomical image of the same subject, and this was then used to transform the individual CBF maps of both the resting state and task-induced data to the high-resolution 3D anatomical space of that subject; second, a non-linear transformation was used to co-register the high-resolution 3D anatomical image of each subject to the common brain MNI-1mm template, which enabled warping of all the transformed maps of a subject to the common brain space. Tri-linear interpolation was employed for image re-gridding in the common 3D space. All group analysis was performed in the common space and regional CBF significantly altered by both anesthetics was overlaid on the high resolution anatomical image and presented in this composite space. The difference between the baseline CBF in the awake state and with propofol (δCBF) was calculated to determine the effect of propofol on baseline activity. Areas where cerebral blood flow was significantly altered from baseline ($p < 0.05$) were defined. The Talairach atlas was then used to identify these regions, and they are listed in Table 1.

Discharge Criteria

After the anesthesia cycle imaging, the propofol infusion was discontinued and subjects were brought out of the scanner. They were transferred to a stretcher and observed for 45 minutes to ensure they met the criteria for discharge. Criteria for discharge were the same as those used in the Yale New Haven Hospital ambulatory surgery unit, including stable vital signs, awake, alert, talking, and ambulating without support (ASA standard

practice). The IV cannulas were then removed from their arms and they were sent home with a responsible adult. Subjects were advised to not drive for the following 24 hours.

Table 1. Various anatomical regions where rCBF was significantly altered from baseline with 2 μg/mL propofol anesthesia.

Anatomical Regions			Talairach Coordinates			Volume (mm3)
	Lobe	**Region**	**X**	**Y**	**Z**	
Right	Parietal Lobe	Postcentral Gyrus	44	-36	60	909
Right	Frontal Lobe	Precentral Gyrus	58	-6	44	348
Right	Parietal Lobe	Postcentral Gyrus	18	-34	60	341
Right	Frontal Lobe	Precentral Gyrus	58	-3	45	3182
Right	Parietal Lobe	Inferior Parietal Lobule	45	-41	55	17732
Left	Frontal Lobe	Middle Frontal Gyrus	-27	25	47	5379
Left	Frontal Lobe	Superior Frontal Gyrus	-36	35	32	12137
Right	Frontal Lobe	Middle Frontal Gyrus	38	54	-7	18523
Right	Frontal Lobe	Middle Frontal Gyrus	36	54	-9	12103
Left	Frontal Lobe	Inferior Frontal Gyrus	-26	15	-14	655
Right	Frontal Lobe	Subcallosal Gyrus	24	8	-13	55
Left	Occipital Lobe	Cuneus	-2	-92	0	5989
Left	Occipital Lobe	Cuneus	-2	-92	2	25794
Left	Occipital Lobe	Middle Occipital Gyrus	-27	-84	13	21292
Left	Temporal Lobe	Fusiform Gyrus	-53	-34	-21	7224
Right	Temporal Lobe	Middle Temporal Gyrus	62	-39	-14	5483
Left	Temporal Lobe	Superior Temporal Gyrus	-62	-18	3	318
Right	Limbic Lobe	Posterior Cingulate	4	-44	24	10310
Right	Limbic Lobe	Posterior Cingulate	3	-41	22	381
Right	Limbic Lobe	Posterior Cingulate	7	-51	25	10290
Left	Frontal Lobe	Medial Frontal Gyrus	-3	41	-9	748
Right	Temporal Lobe	Middle Temporal Gyrus	62	-40	-13	9710
Right	Temporal Lobe	Superior Temporal Gyrus	34	13	-32	3007
Right	Parietal Lobe	Precuneus	41	-72	42	14419
Right	Parietal Lobe	Precuneus	41	-72	41	1081
Left	Sub-lobar	Extra-Nuclear	-35	-24	4	129

Left	Frontal Lobe	Middle Frontal Gyrus	-48	24	23	1101
Left	Frontal Lobe	Middle Frontal Gyrus	-51	24	22	1822
Right	Frontal Lobe	Middle Frontal Gyrus	38	39	23	6240
Right	Frontal Lobe	Middle Frontal Gyrus	47	46	-8	6577
Right	Sub-lobar	Thalamus	14	-23	16	2233
Right	Sub-lobar	Lentiform Nucleus	31	-19	5	98
Right	Sub-lobar	Medial Dorsal Nucleus	7	-18	10	13119
Right	Limbic Lobe	Cingulate Gyrus	1	-8	44	119
Left	Limbic Lobe	Cingulate Gyrus	-4	10	33	64
Inter	Hemispheric	Corpus Callosum	1	18	16	1200
Right	Limbic Lobe	Parahippocampal Gyrus	19	-23	-15	4257
Left	Limbic Lobe	Parahippocampal Gyrus	-15	-15	-15	693
Right	Limbic Lobe	Posterior Cingulate	4	-45	20	32

RESULTS

Thirty healthy ASA I volunteers were studied. There were 17 men and 13 women and their average age was 23 years. Their mean height, body weight, and body mass index were 170.2 cm, 68.8 kg and 23.73 kg/m^2, respectively. Their vital signs, including their heart rate, mean arterial pressure and end tidal CO_2 were all within physiological range during the course of the study, as seen in Table 2. All subjects completed the study successfully without any complications and were discharged within 30 to 45 minutes after completion of the study.

Table 2. Illustrates the mean ± standard deviation oxygen saturation (SpO2), end tidal carbon dioxide (ET-CO2), respiratory rate (RR), systolic blood pressure (SBP), diastolic blood pressure (DBP), mean arterial pressure (MAP), and heart rate (HR) in all subjects at baseline and during 2 μg/mL propofol anesthesia.

	Baseline	2 μg/mL Propofol
SpO_2 (%)	99 ± 1	98 ± 1
ET-CO_2 (mmHg)	34 ± 5	34 ± 6
RR (bpm)	14 ± 2	15 ± 3
SBP (mmHg)	110 ± 10	102 ± 9
DBP (mmHg)	64 ± 8	55 ± 9
MAP (mmHg)	79 ± 8	71 ± 8
HR (bpm)	59 ± 9	62 ± 10

Neurologic Status

With 2 μg/mL propofol, all subjects were asleep and not responding to verbal command. The lowest OAAS score, as described in Figure 2, during propofol anesthesia was 3/5 [37]. No subjects had any recollection of the anesthesia state at the end of the study.

Effect of 2 μg/mL Propofol on baseline CBF

The difference between baseline CBF in the awake state and with propofol in the various anatomical regions (δCBF) is shown in Tables 3 and 4. The δCBF was non-uniform in various anatomical regions, with some areas experiencing a decrease in rCBF and others experiencing an increase. Specifically, the posterior cingulate, thalamus, lentiform nucleus, medial dorsal nucleus, and several areas within the frontal, parietal, temporal, and occipital lobes had a significant decrease in rCBF under propofol anesthesia. In contrast, the cingulate gyrus, parahippocampal gyrus, posterior cingulate, and the corpus callosum had an increase in rCBF under propofol anesthesia. Figure 3 shows the averaged rCBF at baseline in all subjects, while Figure 4 shows the averaged rCBF with 2 μg/mL propofol anesthesia. Figure 5 shows the image of propofol-induced changes in rCBF, illustrating those areas with a significant change in CBF ($p<0.05$). Figure 6 highlights these changes within the thalamus. Thalamic activity correlates with loss of consciousness under anesthesia.

Table 3. δCBF in the various anatomical regions where rCBF significantly decreased with 2 μg/mL propofol anesthesia ($p < 0.05$).

Anatomical Regions			Talairach Coordinates	Vol. (mm^3)	δCBF (ml /100g /min)
	Lobe	Region			
Right	Frontal Lobe	Precentral Gyrus	(58, -6, 44)	909	-8.7
Right	Frontal Lobe	Precentral Gyrus	(58, -3, 45)	3182	-9.2
Right	Frontal Lobe	Middle Frontal Gyrus	(38, 54, -7)	18523	-14.9
Right	Frontal Lobe	Middle Frontal Gyrus	(36, 54, -9)	12103	-14.9
Right	Frontal Lobe	Middle Frontal Gyrus	(38, 39, 23)	6240	-12.0
Right	Frontal Lobe	Middle Frontal Gyrus	(47, 46, -8)	6577	-11.7
Right	Frontal Lobe	Subcallosal Gyrus	(24, 8, -13)	55	-8.6

Left	Frontal Lobe	Middle Frontal Gyrus	(-27, 25, 47)	5379	-10.0
Left	Frontal Lobe	Middle Frontal Gyrus	(-48, 24, 23)	1101	-9.2
Left	Frontal Lobe	Middle Frontal Gyrus	(-51, 24, 22)	1822	-8.3
Left	Frontal Lobe	Medial Frontal Gyrus	(-3, 41, -9)	748	-3.0
Left	Frontal Lobe	Superior Frontal Gyrus	(-36, 35, 32)	12137	-10.3
Left	Frontal Lobe	Inferior Frontal Gyrus	(-26, 15, -14)	655	-6.9
Right	Parietal Lobe	Postcentral Gyrus	(44, -36, 60)	909	-2.9
Right	Parietal Lobe	Postcentral Gyrus	(18, -34, 60)	341	-8.7
Right	Parietal Lobe	Inferior Parietal Lobule	(45, -41, 55)	17732	-10.5
Right	Parietal Lobe	Precuneus	(41, -72, 42)	14419	-9.5
Right	Parietal Lobe	Precuneus	(41, -72, 41)	1081	-9.6
Right	Temporal Lobe	Superior Temp. Gyrus	(34, 13, -32)	3007	-11.3
Right	Temporal Lobe	Middle Temporal Gyrus	(62, -40, -13)	9710	-6.1
Right	Temporal Lobe	Middle Temporal Gyrus	(62, -39, -14)	5483	-11.1
Left	Temporal Lobe	Superior Temp. Gyrus	(-62, -18, 3)	318	-5.4
Left	Temporal Lobe	Fusiform Gyrus	(-53, -34, -21)	7224	-10.6
Left	Occipital Lobe	Cuneus	(-2, -92, 0)	5989	-13.5
Left	Occipital Lobe	Cuneus	(-2, -92, 2)	25794	-13.7
Left	Occipital Lobe	Middle Occipital Gyrus	(-27, -84, 13)	21292	-9.9
Right	Limbic Lobe	Posterior Cingulate	(4, -44, 24)	10310	-10.5
Right	Limbic Lobe	Posterior Cingulate	(3, -41, 22)	381	-11.2
Right	Limbic Lobe	Posterior Cingulate	(7, -51, 25)	10290	-11.6
Right	Sub-lobar	Thalamus	(14, -23, 16)	2233	-4.4
Right	Sub-lobar	Lentiform Nucelus	(31, -19, 5)	98	-4.3
Right	Sub-lobar	Medial Dorsal Nucleus	(7, -18, 10)	13119	-12.2
Left	Sub-lobar	Extra-Nuclear	(-35, -24, 4)	129	-7.2

Table 4. δCBF in the various anatomical regions where rCBF significantly increased with 2 μg/mL propofol anesthesia ($p < 0.05$).

Anatomical Regions			**Talairach Coordinates**	**Vol. (mm^3)**	**δCBF (ml /100g /min)**
	Lobe	**Region**			
Right	Limbic Lobe	Cingulate Gyrus	(1, -8, 44)	119	4.5
Right	Limbic Lobe	Parahippocampal Gyrus	(19, -23, -15)	4257	14.8
Right	Limbic Lobe	Posterior Cingulate	(4, -45, 20)	32	5.6
Left	Limbic Lobe	Cingulate Gyrus	(-4, 10, 33)	64	3.2
Left	Limbic Lobe	Parahippocampal Gyrus	(-15, -15, -15)	693	2.6
Inter	Hemispheric	Corpus Callosum	(1, 18, 16)	1200	5.9

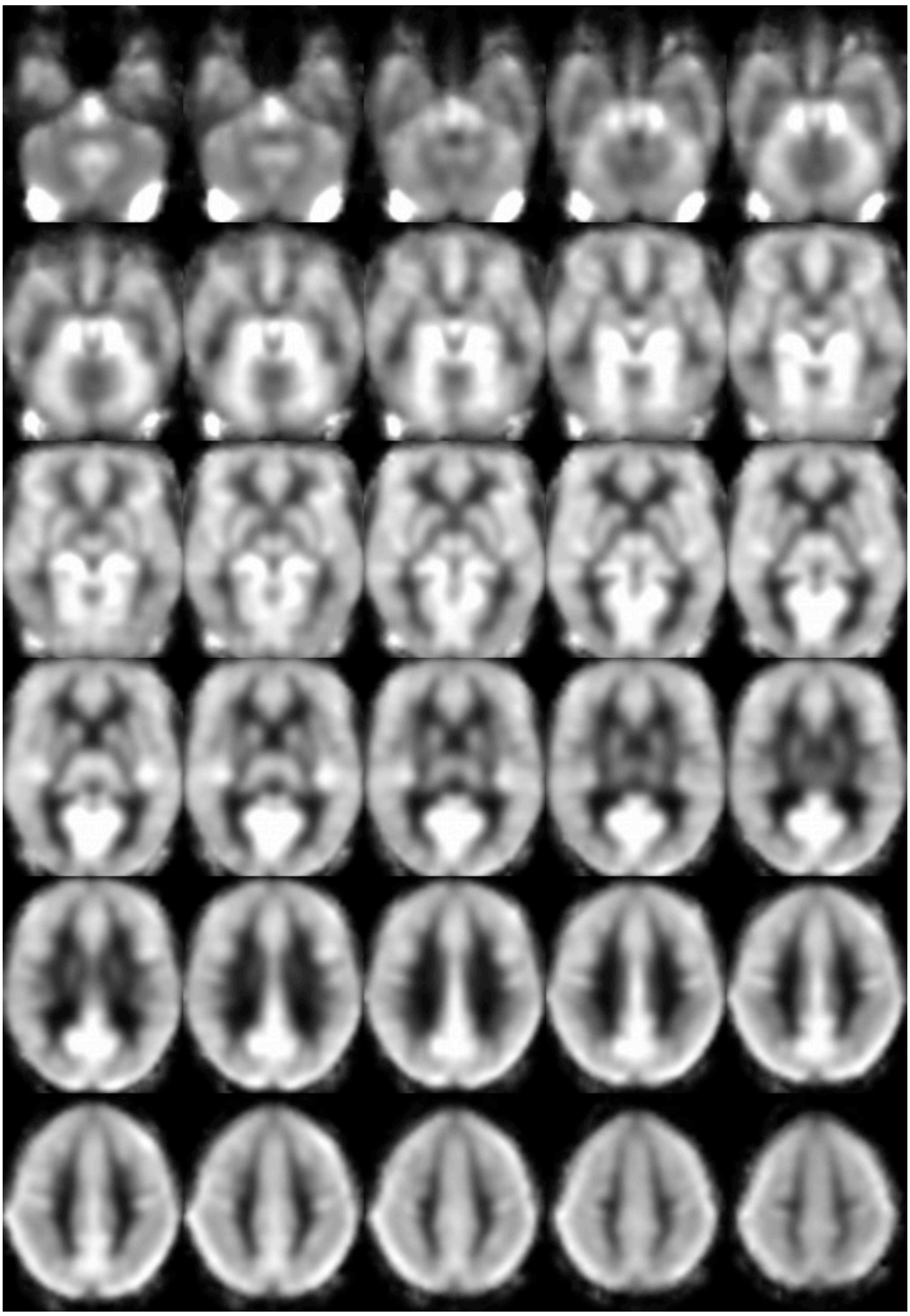

Figure 3. Illustrates the averaged baseline regional cerebral blood flow before anesthesia in all subjects.

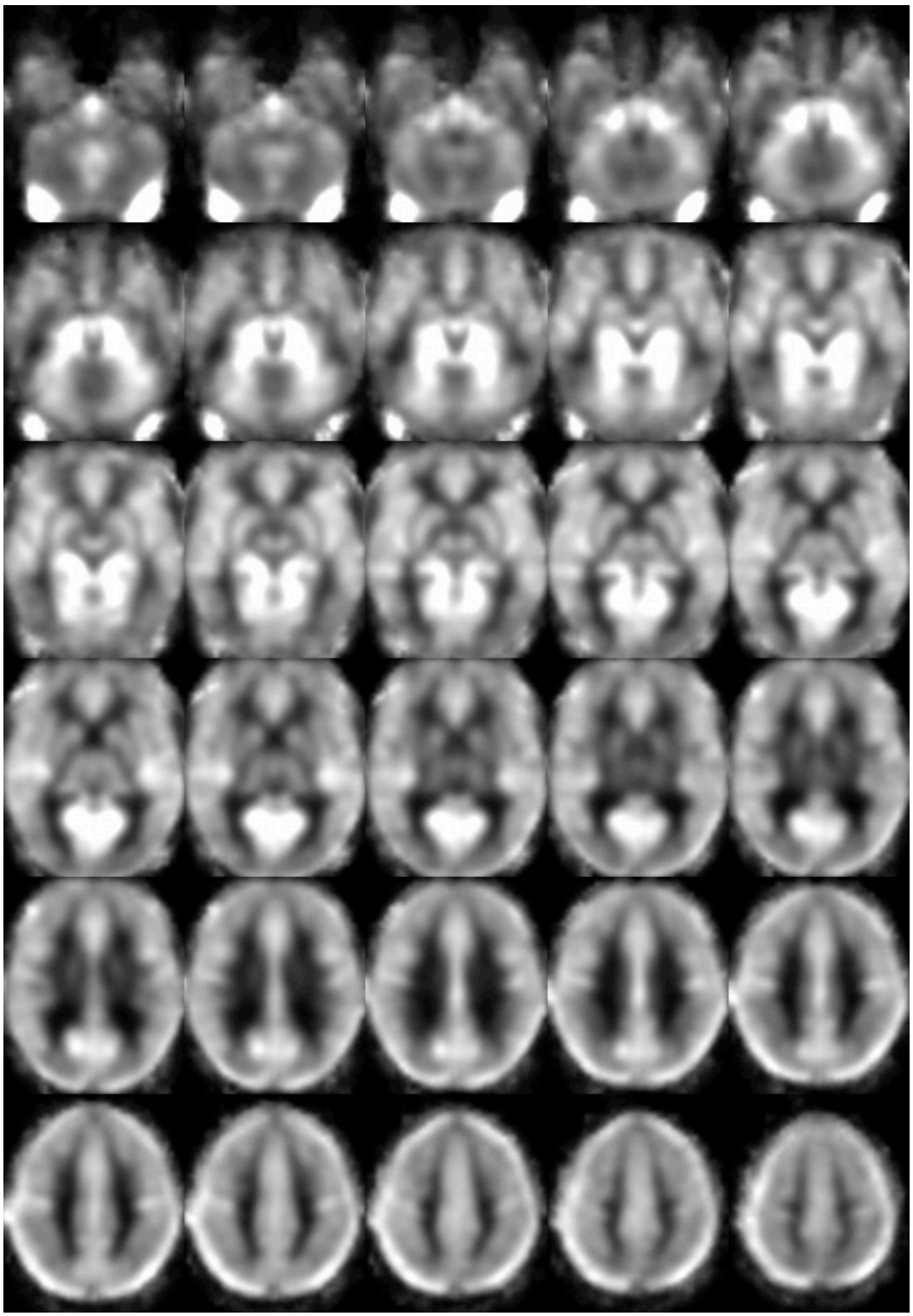

Figure 4. Illustrates the averaged regional cerebral blood flow (rCBF) with propofol 2 μg/ml in all subjects.

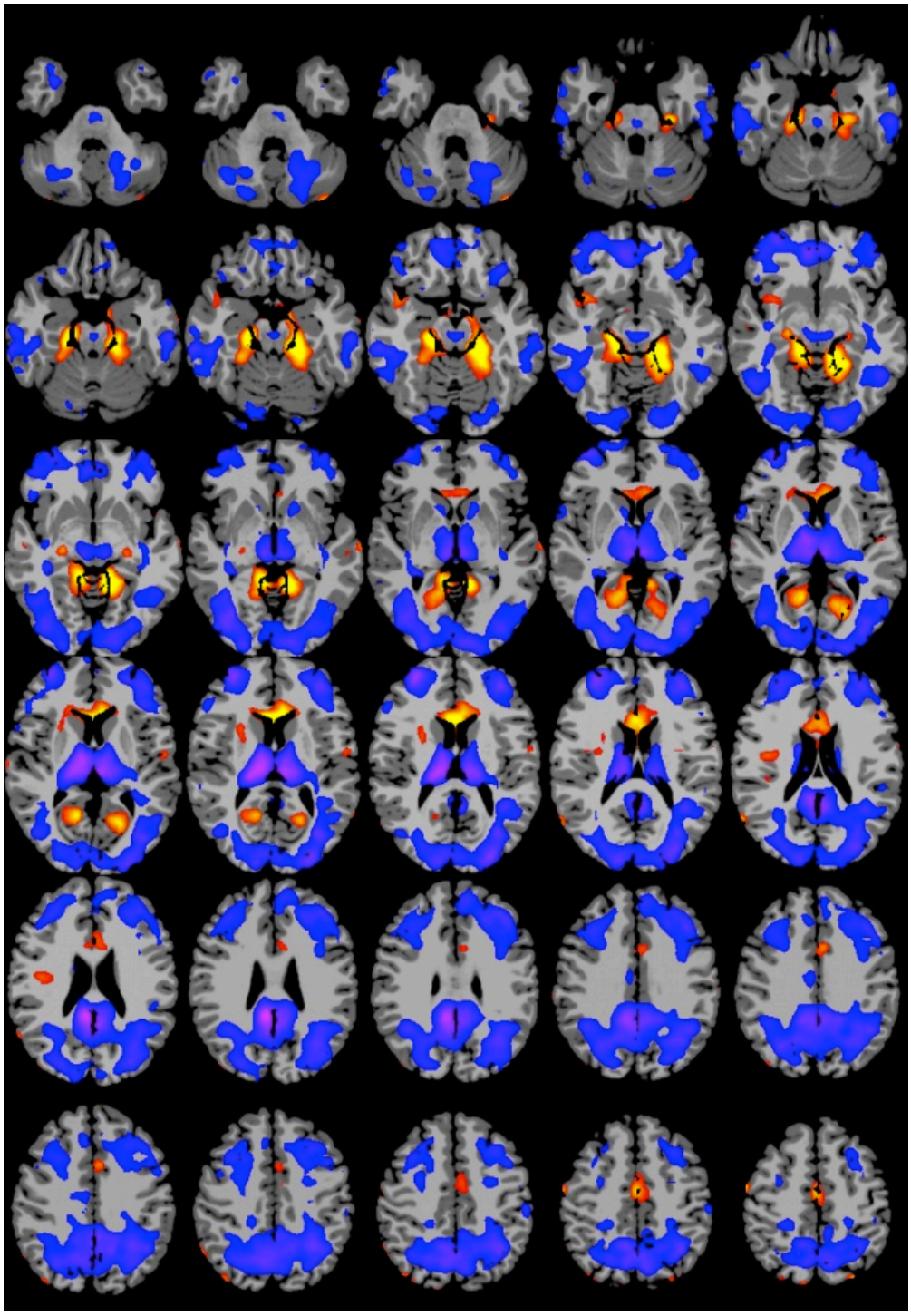

Figure 5. Illustrates the averaged change in regional cerebral blood flow (δCBF) with propofol 2 μg/ml in various voxels of the brain. Red/orange areas imply an increase in rCBF and purple/blue areas reflect a decrease in rCBF ($p < 0.05$).

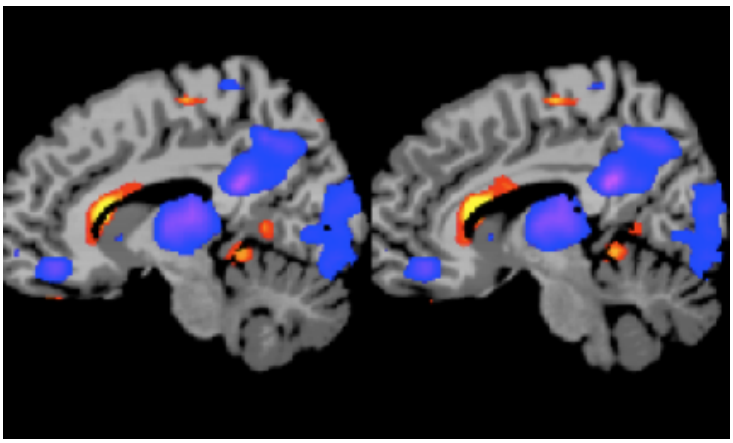

Figure 6. Illustrates the change in regional cerebral blood flow (δCBF) with propofol 2 μg/ml within the thalamus. Red/orange areas imply an increase in rCBF and purple/blue areas reflect a decrease in rCBF ($p < 0.05$).

Comparison of changes in rCBF in propofol vs. sevoflurane 0.5 MAC anesthesia

The measured δCBF with 0.5 MAC equivalent propofol anesthesia was then compared qualitatively to that observed with 0.5 MAC sevoflurane. Tables 5 and 6 illustrate δCBF in the various anatomical regions where rCBF decreased and increased, respectively, with 0.5 MAC sevoflurane. Areas with a significant decrease in rCBF include the anterior cingulate, cingulate gyrus, lentiform nucleus, thalamus, and cerebellum, as well as areas within the frontal, parietal, temporal, and occipital lobes. In contrast, areas with a significant increase in rCBF with 0.5 MAC sevoflurane include the superior temporal gyrus, anterior cingulate, cingulate gyrus, claustrum, insula, and pons.

Table 5. δCBF in the various anatomical regions where rCBF significantly decreased under 0.5 MAC sevoflurane anesthesia ($p < 0.05$). Data provided courtesy of Ramachandran Ramani, Yale School of Medicine, and adapted for comparison.

Anatomical Regions			Talairach Coordinates	δCBF (ml/100g/min)
	Lobe	**Region**		
Right	Frontal Lobe	Middle Frontal Gyrus	(30, 34, -8)	-9
Right	Frontal Lobe	Middle Frontal Gyrus	(34, 24, 40)	-9
Right	Frontal Lobe	Medial Frontal Gyrus	(13, 45, 4)	-11
Right	Frontal Lobe	Subcallosal Gyrus	(12, 11, -11)	-12
Left	Frontal Lobe	Middle Frontal Gyrus	(-28, 35, -13)	-20
Left	Frontal Lobe	Middle Frontal Gyrus	(-42, 29, 39)	-11
Left	Frontal Lobe	Subgyral	(-11, 34, -14)	-18
Right	Parietal Lobe	Inferior Parietal Lobule	(60, -27, 29)	-10
Right	Parietal Lobe	Inferior Parietal Lobule	(53, -40, 40)	-9
Left	Parietal Lobe	Inferior Parietal Lobule	(-61, -30, 28)	-13
Left	Parietal Lobe	Inferior Parietal Lobule	(-55, -37, 40)	-9
Right	Temporal Lobe	Superior Temporal Gyrus	(33, 10, -38)	-13
Left	Temporal Lobe	Superior Temporal Gyrus	(-31, 5, -31)	-20
Left	Occipital Lobe	Cuneus	(-2, -97, 3)	-17
Right	Limbic Lobe	Anterior Cingulate	(11, 44, 3)	-12
Left	Limbic Lobe	Cingulate Gyrus	(-1, -26, 28)	-20
Left	Sub-lobar	Lentiform Nucleus	(-14, 11, -10)	-21
Right	Thalamus	Medial Dorsal Nucleus	(8, -21, 10)	-9
Right	Thalamus	Ventral Anterior Nucleus	(7, -13, 16)	-10
Left	Thalamus	Medial Dorsal Nucleus	(-8, -21, 8)	-10
Left	Thalamus	Ventral Anterior Nucleus	(-9, -13, 15)	-9
Right	Cerebellum	Pyramis	(39, -77, -33)	-20
Right	Cerebellum	Cerebellar Tonsil	(44, -51, -33)	-33
Left	Cerebellum	Pyramis	(-47, -70, -33)	-14
Left	Cerebellum	Cerebellar Tonsil	(-42, -49, -34)	-16
Left	Cerebellum	Culmen	(-4, -49, -9)	-11

Table 6. δCBF in the various anatomical regions where rCBF significantly increased under 0.5 MAC sevoflurane anesthesia ($p < 0.05$). Data provided courtesy of Ramachandran Ramani, Yale School of Medicine, and adapted for comparison.

Anatomical Regions			Talairach Coordinates	δCBF (ml/100g/min)
	Lobe	**Region**		
Right	Temporal Lobe	Superior Temporal Gyrus	(41, 2, -19)	9
Right	Temporal Lobe	Middle Temporal Gyrus	(62, -39, -7)	13
Left	Temporal Lobe	Superior Temporal Gyrus	(-50, 1, -7)	12
Left	Temporal Lobe	Middle Temporal Gyrus	(-41, 2, -20)	10
Left	Temporal Lobe	Middle Temporal Gyrus	(-42, 0, -25)	12
Right	Occipital Lobe	Lingual Gyrus	(22, -59, 3)	11
Right	Limbic Lobe	Parahippocampal Gyrus	(21, -27, -7)	11
Right	Limbic Lobe	Parahippocampal Gyrus	(21, -44, -6)	11
Right	Limbic Lobe	Parahippocampal Gyrus	(14, -44, 0)	10
Right	Limbic Lobe	Anterior Cingulate	(0, 30, 4)	9
Left	Limbic Lobe	Parahippocampal Gyrus	(-31, -21, -23)	11
Left	Limbic Lobe	Parahippocampal Gyrus	(-24, -26, -9)	11
Left	Limbic Lobe	Parahippocampal Gyrus	(-27, -43, -7)	9
Left	Limbic Lobe	Parahippocampal Gyrus	(-19, -44, 0)	11
Left	Limbic Lobe	Cingulate Gyrus	(-1, 15, 29)	8
Right	Sub-lobar	Claustrum	(37, 1, -8)	12
Right	Sub-lobar	Insula	(39, 5, -1)	11
Left	Sub-lobar	Insula	(-39, 6, 0)	9
Right	Brainstem	Pons	(9, -16, -19)	18

DISCUSSION

The present study address three main questions:

1) How does 0.5 MAC equivalent propofol anesthesia affect regional cerebral blood flow and thus regional neuronal activity?

2) How do these changes compare to that observed with 0.5 MAC sevoflurane anesthesia in an earlier study?

3) What is the neurophysiological significance of the observed changes in regional cerebral blood flow?

Our results clearly illustrate that propofol causes a non-uniformity in rCBF. Regions manifesting a rise in rCBF include the cingulate gyrus, parahippocampal gyrus, posterior cingulate, and the corpus callosum. Regions manifesting a decrease in rCBF include several areas within the frontal, parietal, temporal, and occipital lobes, as well as the posterior cingulate, thalamus, lentiform nucleus, and medial dorsal nucleus.

Effects of propofol on the frontal lobe

Within the frontal lobe, propofol caused the most drastic decrease in CBF in bilateral middle frontal gyri in addition to the left medial frontal gyrus, left superior frontal gyrus, left inferior frontal gyrus, right precentral gyrus, and right subcallosal gyrus (Figure 7). No regions within the frontal lobe had a significant increase in regional cerebral blood flow. The frontal lobe is implicated in higher order processing functions of the brain, including executive functions and emotional memories linked with the limbic system, as well as in the control of autonomic responses [44, 45]. It receives input from the dorsomedial thalamic nucleus [46].

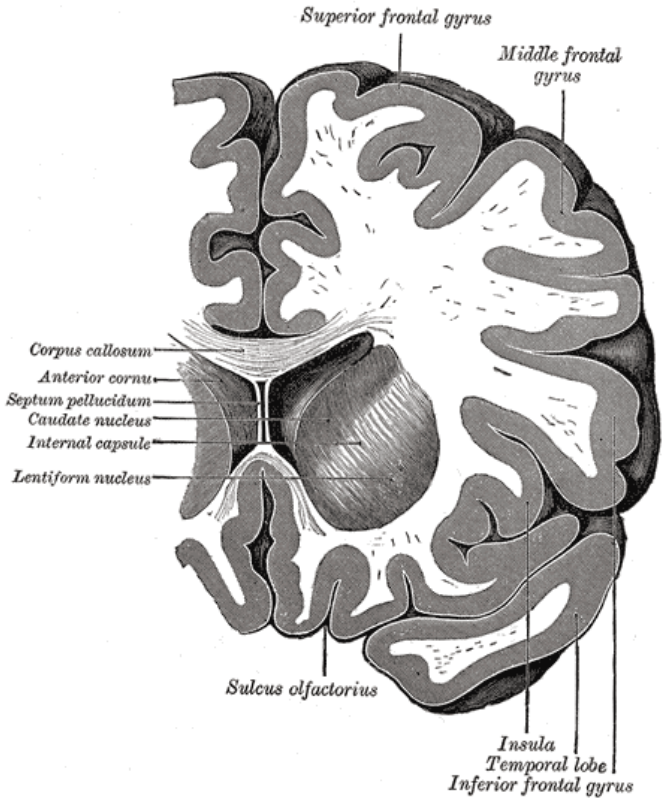

Figure 7. Coronal section through the anterior horn of the lateral ventricles. Illustrates the superior, middle, and inferior frontal gyri [47].

Studies looking at the action of middle frontal gyrus have found it to play a critical role in both the storage and processing components of working memory in the brain [46, 48]. It is part of the prefrontal cortex (PFC) and constitutes one third of the frontal lobe. Thus, it can be inferred that propofol impairs working memory by decreasing its capacity. The dorsolateral prefrontal cortex (DLPFC) forms the middle third of the middle frontal gyrus and is deactivated in REM sleep. The superior frontal gyrus is involved in self-awareness, working with the sensory system [49]. In contrast, the inferior frontal gyrus has different roles in each hemisphere. The right inferior frontal

gyrus plays a role in risk aversion while the left inferior frontal gyrus, also known as Broca's area, plays a critical role in language production and verb comprehension [50, 51]. This is consistent with previous findings showing the impaired recognition memory and verbal memory caused by propofol [52, 53]. It is important to note that significant decreases in cerebral blood flow with 0.5 MAC propofol anesthesia was only noted in the left inferior frontal gyrus and left superior frontal gyrus, indicating that these regions are more susceptible to the effects of propofol. It has been implicated the propofol may specifically and preferentially affect higher processing areas of the brain, such as the frontal and temporal lobe, and our results reaffirm this theory [3].

Effects of propofol on the parieto-occipito cortex

The parieto-occipito cortex was another cortical region particularly affected by propofol. Specifically, the right precuneus, right inferior parietal lobule, right postcentral gyrus, left cuneus and left middle occipital gyrus had significant decreases in rCBF. The inferior parietal lobule is located below the horizontal portion of the intraparietal sulcus and behind the lower portion of the posterior central sulcus. It is concerned with the perception of facial emotions and in sensory information interpretation [54]. It is also connected with language, mathematical operations, and body image.

The cuneus and precuneus are involved in basic visual processing, episodic memory, and aspects of consciousness [21]. The cuneus is a wedge shaped portion of the occipital lobe seen predominantly on the medial side of the sagittal section of the brain. The left cuneus receives information from the inferior part of the right visual field and vice versa. Evidence suggests that the precuneus plays a pivotal role in self-awareness

and in producing a conscious self-percept [55]. PET studies have shown that alterations in activity of the middle occipital lobe, cuneus, and precuneus modulate the level of consciousness, with propofol leading to a deactivation in these areas [23, 56, 57]. Similarly, in our study, propofol led to a decrease in rCBF in these areas, suggesting that deactivation in these regions of the parieto-occipito cortex is important in achieving the pharmacological effects of propofol.

Effects of propofol on the temporal lobe

In the temporal lobe, bilateral superior temporal gyri as well as areas in the right middle temporal gyrus showed a significant decrease in rCBF from baseline with propofol. The superior temporal gyrus is involved in the sensation of sound as well as in the processing of speech, as it contains the primary auditory cortex as well as Wernicke's area [58]. In addition, this area has been implicated in the perception of emotion in facial expressions, as has the middle temporal gyrus [54]. Changes in regional cerebral blood flow to the temporal lobe perhaps reflect the breakdown of the language processing networks under propofol-induced anesthesia [59]. Functional imaging techniques have previously shown propofol to disrupt connections from the primary auditory cortex to the frontal regions and the thalamus [60].

Effects of propofol on the limbic lobe

The limbic lobe is a C-shaped structure of the medial hemispheric surface, consisting of parts of the frontal, parietal, and temporal lobes. It encircles the corpus callosum and the lateral aspect of the midbrain, and includes the cingulate gyrus,

parahippocampal gyrus, hippocampal formation, paraterminal gyrus and subcallosal area (Figure 8). The limbic lobe plays a central role in memory, emotional processing, and in affective behaviors with strong emotional content [61].

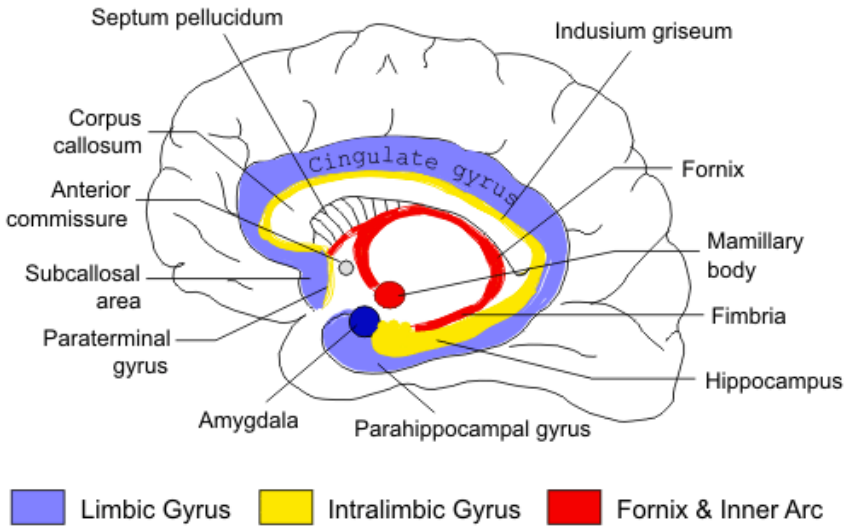

Figure 8. Sagittal illustration of the brain highlighting key areas of the limbic lobe, including the subcallosal area, cingulate gyrus, hippocampal formation, and parahippocampal gyrus. Adapted from Hesslink JR (2011) [62].

In the limbic lobe, both significant decreases and increases in rCBF were observed. A decrease in rCBF was seen in the right posterior cingulate, while increases in rCBF occurred in bilateral parahippocampal gyri, bilateral cingulate gyri, and the right posterior cingulate. The posterior cingulate has been found to be functionally heterogeneous, and is implicated to play a role in pain processing and episodic memory retrieval, as well as serve as one of the neural substrates for human awareness [63]. It receives information from the thalamus and neocortex, and relays it to the entorhinal

cortex located in the medial temporal lobe. Together with the precuneus, the posterior cingulate cortex plays a pivotal role in conscious information processing. These regions have the highest level of metabolism in the human brain and form part of the neural network correlates of consciousness (NNCC) [64]. PET studies looking at rCBF with propofol have also shown a decrease in activity in the precuneus and posterior cingulate cortex with deepening of propofol-induced sedation, followed by a complete restoration of activity in these areas upon the return of consciousness [23, 65]. In our study, it was the only area within the limbic lobe that showed a decrease in rCBF, though there was a region in the right posterior cingulate and left cingulate gyrus that had an increase in rCBF. There was also an increase in rCBF in the parahippocampal gyrus, which plays an important role in memory encoding and retrieval. Increased activity in this area with anesthesia is intriguing and must be further investigated. Studies have shown that stimulation in the area is able to produce complex visual hallucinations and is associated with auditory hallucinations in schizophrenic patients [66].

Effects of propofol on subcortical areas

A recent study by Sun et al. looked at changes in cerebral glucose metabolism using PET at two different doses of propofol. Whole brain glucose metabolism was reduced in the cortical areas at the lower dose (1.5 μg/ml), but also occurred in the subcortical areas with the higher dose of propofol (2.5 μg/ml) [67]. This is consistent with previous propofol studies reporting decreased activity in the cortical area more than in subcortical areas [14, 67]. We found similar results, with propofol having a greater effect on cortical areas. In terms of subcortical regions, we observed a decrease in rCBF

in the right lentiform nucleus and right thalamus, including the medial dorsal nucleus, with 0.5 MAC equivalent propofol. The lentiform nucleus encompasses the putamen and globus pallidus in the basal ganglia, which plays an important role in regulating movement on a minute-to-minute basis.

Effects of propofol on the thalamus

The thalamus is typically thought to serve as the relay station of the brain, processing sensory information and relaying it to different parts of the brain. In addition, it plays a critical role in the maintenance of consciousness and in regulating the sleep and wakeful states, suggesting that thalamic deactivation may play a central role in anesthesia-induced loss of consciousness [23, 68]. It is important to note that while we observed a decrease in rCBF in both the right and left thalamus, the decrease was only significant on the right (Figure 6).

Numerous previous studies investigating the effects of propofol on rCBF have also shown a dramatic reduction in blood flow to the thalamus under anesthesia [3, 18, 65, 69]. Electrophysiological studies looking at thalamocortical interactions have found them to be decreased in natural sleep as well as under anesthesia [23]. The medial dorsal nucleus of the thalamus, which plays a role in memory, attention, planning, and receives dense inputs from the prefrontal cortex and limbic system, has also been found to be preferentially sensitive to the effects of propofol, as was found in the present study [69]. In addition, these previous studies too have noted that the effects of propofol preferentially decreases rCBF in the right thalamus in comparison to the left, but the significance of this remains unknown [23, 65, 69]. It has been suggested that decreases

in rCBF to the thalamus may be due to the decreased activity of the cortex under anesthesia, thus decreasing corticothalamic inputs, and we cannot rule this out as a contributing factor [69].

Comparison of effects of sevoflurane and propofol

With 0.5 MAC sevoflurane anesthesia, there was also a non-uniformity in rCBF, as has previously been seen with 0.25 MAC sevoflurane [70]. Regions manifesting a rise in rCBF include the superior temporal gyrus, middle temporal gyrus, lingual gyrus, parahippocampal gyrus, anterior cingulate, cingulate gyrus, claustrum, insula, and pons. Regions manifesting a decrease in rCBF with sevoflurane anesthesia include areas within the frontal, parietal, temporal, and occipital lobes, as well as the anterior cingulate, cingulate gyrus, lentiform nucleus, thalamus, and cerebellum.

Frontal lobe

In terms of the frontal lobe, both propofol and sevoflurane caused a decrease in rCBF in many areas modulating higher order mental functions, including the middle frontal gyrus, medial frontal gyrus, and subcallosal gyrus, indicating that these regions may play a critical role in the action of anesthetic agents. Given the role these regions play in the storage and processing of working memory, as well as in executive function, perhaps suppressing the action of these areas helps to induce the amnesic effects of anesthesia.

Parieto-occipito lobe

Both sevoflurane and propofol also caused a decrease in rCBF to the inferior parietal lobule and the cuneus area, but sevoflurane did not lead to a decrease in rCBF in the precuneus. Thus, perhaps the precuneus area is specifically targeted by propofol and contributes to a decreased level of consciousness and arousal experienced with the anesthetic agent. The occipital lobe does have a higher concentration of GABA receptors compared to other areas of the brain, which may help explain why propofol causes a decrease in rCBF but sevoflurane does not. Further studies looking at the action of propofol in this area using various receptor ligands are needed to better understand the molecular mechanism of its action in this area.

Temporal lobe

In the temporal lobe, sevoflurane caused both an increase and decrease in rCBF in different voxels of the superior temporal gyrus, and led to an increase in rCBF in the middle temporal gyrus. This is the opposite of that seen with propofol, which led to suppression of the language processing area in the superior temporal gyrus and suppression of the middle temporal gyrus, which is important in recognition of known faces.

Thalamus

Sevoflurane and propofol both led to a decrease in rCBF in the thalamus, though with sevoflurane this occurred bilaterally rather than unilaterally on the right. This reaffirms that the thalamus is a critical site of action for anesthetic agents and is not specific to propofol. Decreased activity within the thalamus as well as the above

mentioned cortical areas, including regions of the temporal lobe, the inferior parietal lobule, and the inferior and middle frontal gyri, have also been identified in association with the decreased level of consciousness seen in sleep and coma [71, 72, 73]. Clinically, our subjects in both studies were asleep with OAA/S scores of 3/5 or less, and they did not have any memory of the events during the anesthesia cycle. However, no specific memory test was carried out.

Limbic lobe

In addition, both sevoflurane and propofol led to an increase in rCBF in the parahippocampal gyrus in the limbic lobe, the significance of which must be further investigated. Whereas propofol led to a decrease in rCBF in the posterior cingulate, sevoflurane led to a decrease in rCBF in the anterior cingulate and cingulate gyrus. This indicates that both agents suppressed areas within the limbic lobe, though their exact targets differed. Whereas the posterior cingulate (main nodal region for default mode network) plays an important role in conscious information processing, the anterior cingulate has important autonomic functions, including regulating blood pressure and heart rate, as well as pain processing and modulation. This may explain why we observed a greater drop in blood pressure and heart rate with sevoflurane anesthesia in comparison to propofol [21, 23]. Nonetheless, further studies are needed in order to justify such an assumption.

Cerebellum

One region that was seemingly unaffected with propofol but had a significant decrease in rCBF with sevoflurane was the cerebellum, which is involved in motor control and coordination. Multiple voxels within both the right and left cerebellum were suppressed with sevoflurane, which may contribute to the decreased muscle tone observed under anesthesia. In contrast, a PET study looking at the effects of propofol on the CNS found an increase in rCBF in the cerebellum, which was attributed to the initial increase in muscle tone and jerking movements seen during the early states of propofol anesthesia [23]. However, we did not observe these changes with propofol. Another PET study found the cerebellum to be easily suppressed by both sevoflurane and propofol, indicating the need for further studies to better understand the effects of anesthesia on this region [74].

PASL Technique

Although studies have been done looking at the cerebral effects of propofol using PET and EEG, this is the first study to our knowledge using PASL cerebral perfusion technique to investigate the effects of propofol anesthesia on the human brain. In order to best interpret our results, it is imperative to understand the biophysical mechanisms of perfusion imaging using pulsed arterial spin labeling (PASL) and its advantages and disadvantages in assessing the effects of propofol and sevoflurane on cerebral blood flow. As stated previously, in the PASL technique, instead of using an extrinsic tracer, a RF pulse sequence is applied to the arterial water spins. By adding the inversion delay, these inverted arterial spins are allowed time to diffuse through the blood-brain barrier, where they are exchanged with the tissue magnetization at the capillary level, reducing its

intensity. The degree to which the spin is attenuated serves as a measure of perfusion to that region [32].

The benefit of this technique is that it is completely noninvasive, does not require injection of contrast, and has a very high spatial and temporal resolution. In addition, it is more accurate at localizing regions of activation, since it is concerned with activity at the capillary level, and not affected by the change in deoxygenated blood in the downstream venous areas as in BOLD [75]. However, some argue that there could be possible confounding factors secondary to changes in physiologic variables caused by the anesthetic agent [59]. For instance, changes in systemic arterial blood pressure with propofol and sevoflurane could decrease CBF. However, studies have shown that changes in blood pressure do not affect CBF so long as the mean arterial pressure is within the autoregulatory range and autoregulation is intact, which is the case for the 0.5 MAC levels of anesthesia used in this study [23, 59]. As shown in Table 2, all physiological parameters (MAP, ET_{CO2}, SpO_2, HR) were within normal limits during the study.

Under normal circumstances in which the MAP between 60 and 150 mmHg, the average cerebral blood flow is relatively constant due to protective autoregulation. Within this range, a fall in cerebral perfusion would lead to vasodilation of the cerebral resistance vessels within seconds, and thus an increase in cerebral blood flow. In contrast, an increase in cerebral perfusion would lead to vasoconstriction, causing an immediate decrease in cerebral blood flow. As stated above, the MAP at baseline for all subjects was 79 ± 8 mmHg, while under anesthesia is was 71 ± 8 mmHg. Both values fall within the autoregulatory range. In addition, there was no significant difference in

the subjects' SpO_2, end tidal CO_2, and heart rate before and after anesthesia was administered. Thus, the observed changes in rCBF can justifiably be attributed to changes in metabolic activity rather than changes in systemic blood pressure.

It has also been argued that sevoflurane is known to have direct cerebral vasodilatory effects, which could alter the rCBF [76]. While this cannot be excluded as a contributing factor, we assume that it only minimally impacts the large changes in rCBF observed in our study and that the net direction of change in rCBF is accurate. Marcar et al. (2006) used fMRI to study the depth of anesthesia on the extent and amplitude of the BOLD response in children, and found that up to 0.5 MAC sevoflurane, vasodilation was not significant [77]. However, beyond 1.0 MAC sevoflurane, vasodilation did become significant [77]. In addition, vasoactive changes would affect global circulation rather than flow in particular regions, thereby lessening any impact on the relative changes observed [23]. Such changes do not occur with propofol, and any changes in rCBF observed can be taken as a direct reflection of changes in neuronal activity induced by the anesthetic agent.

Limitations

One limitation of our study is that we did not look at the concentration dependent effects on the brain, as has previously done with PET imaging [17, 23]. The effects observed in our study were obtained at a single and equivalent dose level of propofol and sevoflurane. Thus, we are not able to determine if certain areas affected by these anesthetic agents are more susceptible to the effects of anesthesia, nor the sequence in

which various cortical and subcortical structures are suppressed. Further studies looking at the concentration dependent effects on rCBF using PASL are needed.

A second limitation of our study is that we did not use any task activation to specifically look at the effects of 0.5 MAC propofol or sevoflurane on a targeted area, such as the visual, auditory, or motor cortex. In order to better determine the extent to which a certain region of the brain is affected by anesthesia, it would be more accurate to measure δCBF during task activation in both the awake and anesthetized states and then look at the difference between the two. By studying both the changes in rCBF with different types of task activation and with various doses of anesthesia, we would be able to more completely understand the anesthetic effects of propofol and sevoflurane on neuronal activity. Nevertheless, our study lays a strong foundation by identifying various regions in the brain that are significantly altered from baseline with propofol and sevoflurane, and that may be further investigated in future studies using different doses and task activation.

A third limitation of our study is that we did not measure metabolism, which would confirm that the CBF changes we observed do truly reflect changes in neuronal activity. However, given that propofol does not have significant vasodilatory effects, the rCBF changes we observed can be taken as a direct reflection of change in neuronal activity.

Conclusions

In summary, this study provides direct imaging evidence showing that propofol preferentially decreases regional cerebral blood flow in a specific set of cortical regions

and the thalamus, similar to those observed with sevoflurane. The loss of consciousness observed with these agents likely correlates with deactivation of the thalamus, though effects on cognitive process involving areas of the frontal, parietal, and temporal lobes likely contribute to this effect. Given that both propofol and sevoflurane potentiate the effects of GABA at the receptor level, areas with a higher concentration of such synapses are expected to be more sensitive to the effects of these anesthetic agents [3, 33]. This may help explain why propofol and sevoflurane preferentially affect these higher processing regions of the brain with more corticocortical connections. However, further studies are needed to understand the mechanism of loss of consciousness induced by propofol and sevoflurane, and to determine if the above mentioned cortical areas are directly or indirectly involved in the process.

REFERENCES

1. Alkire MT, Hudetz AG, Tononi G. Consciousness and anesthesia. *Science* 2008; 322: 876-880.

2. Vasileiou I, Xanthos T, Koudouna E, Perrea D, Klonaris C, Katsargyris A, Papadimitriou L. Propofol: a review of its nonanaesthetic effects. *Eur J Pharmacol* 2009; 605: 1-8.

3. Zhang H, Wang W, Zhao Z, Ge Y, Zhang J, Yu D, Chai W, Wu S, Xu L. The action sites of propofol in the normal brain revealed by functional magnetic resonance imaging. *The Anatomical Record* 2010; 293: 1985-1990.

4. Urban BW. Current assessment of targets and theories of anaesthesia. *Br J Anaesth* 2002; 89: 167-183.

5. Urban BW, Bleckwenn M, Barann M. Interactions of anesthetics with their targets: non-specific, specific, or both? *Pharmacol Ther* 2006; 111: 729-770.

6. Vanlersberghe C and Camu F. Propofol. *Handb Exp Pharmacol* 2008; 227-252.

7. Zhang H, Wang W, Gao W, Ge Y, Zhang J, Wu S, Xu L. Effect of propofol on the levels of neurotransmitters in normal human brain: a magnetic resonance spectroscopy study. *Neurosci Lett* 2009; 467: 247-251.

8. Campagna JA, Miller KW, Forman SA. Mechanisms of actions of inhaled anesthetics. *NEJM* 2003; 348: 2110-2124.

9. Ishizawa Y. Mechanisms of anesthetic actions and the brain. *J Anesth* 2007; 21: 187-199.

10. Schlunzen L, Vafaee MS, Cold GE, Rasmussen M, Nielsen JF, Gjedde A. Effects of subanaesthetic and anaethetic doses of sevoflurane on regional cerebral blood flow in healthy volunteers. A positron emission tomographic study. *Acta Anaethsiol Scand* 2004; 48: 1268-1276.

11. Heinke W and Schwarzbauer C. In vivo imaging of anaesthetic action in humans: approaches with positron emission tomography (PET) and functional magnetic resonance imaging (fMRI). *British Journal of Anaesthesia* 2002; 89(1): 112-122.

12. Fox P, Raichle M, Mintun M, Dence C. Nonoxidative glucose consumption during focal physiologic neural activity. *Science* 1988; 241: 462-464.

13. Ramani R and Wardhan R. Understanding anesthesia through functional imaging. Current Opinions in *Anaesthesiology* 2008; 21: 530-536.

14. Alkire MT, Haier RJ, Barker SJ, et al. Cerebral metabolism during Propofol anesthesia in humans studied with positron emission tomography. *Anesthesiology* 1995; 82: 393-403.

15. Alkire MT, Haier RJ, Shah NK, Anderson CT. Positron emission tomography study of regional cerebral metabolism in humans during isoflurane anesthesia. *Anesthesiology* 1997; 86: 549-557.

16. Alkire MT, Pomfrett CJ, Haier RJ, et al. Functional brain imaging during halothane anesthesia in humans: effects of halothane on global and regional cerebral glucose metabolism. *Anesthesiology* 1999; 90: 701-709.

17. Schlunzen L, Cold GE, Rasmussen M, Vafaee MS. Effects of dose-dependent levels of isoflurane on cerebral blood flow in healthy subjects studied using positron emission tomography. *Acta Anaesthesiol Scand* 2006; 50: 306-312.

18. Schlunzen L, Juul N, Hansen KV, Cold GE. Regional cerebral blood flow and glucose metabolism during propofol anaesthesia in healthy subjects studied with positron emission tomography. *Acta Anaestheiol Scand* 2011; 1-8. [E-pub ahead of print]

19. Franks NP, Lieb WR. Molecular and cellular mechanisms of general anesthesia. *Nature* 1994; 367: 607-614.

20. Lees G. Molecular mechanisms of anaesthesia: light at the end of the channel? *British Journal of Anaesthesia* 1998; 81: 491-493.

21. Kaisti KK, Metsahonkala L, Teras M, OIkonen V, Aalto S, Jaaskelainen S, Hinkka S, Scheinin H. Effects of surgical levels of Propofol and sevoflurane anesthesia on cerebral blood flow in health subjects studied with positron emission tomography. *Anesthesiology* 2002; 96: 1358-70.

22. Kaisti KK, Langsjo JW, Aalto S, Oikonen V, Sipilia H, Teras M, Hinkka S, Metsahonkala L, Scheinin H. Effects of sevoflurane, Propofol, and adjunct nitrous oxide on regional cerebral blood flow, oxygen consumption, and blood volume in humans. *Anesthesiology* 2003; 99: 603-613.

23. Fiset P, Paus T, Daloze T, Plourde G, Meuret P, Bonhomme V, Hajj-Ali N, Backman SB, Evans AC. Brain mechanisms of Propofol-induced loss of consciousness in humans: a positron emission tomographic study. *The Journal of Neuroscience* 1999; 19(13): 5506-5513.

24. Ludbrook GL, Upton RN, Grant C, Gray EC. Cerebral effects of propofol following bolus administration in sheep. *Anaesth Intensive Care* 1996; 24: 26-31.

25. Heinke W and Schwarzbauer C. Subanesthetic isoflurane affects task-induced brain activation in a highly specific manner. A functional magnetic resonance imaging study. *Anesthesiology* 2001; 94: 973-981.

26. Berns GS. Functional neuroimaging. *Life Sciences* 1999; 65(24): 2531-2540.

27. Ogawa S, Lee TM, Kay AR, Tank DW. Brain magnetic resonance imaging with contrast dependent on blood oxygenation. *Proc Natl Acad Sci* 1990; 87: 9868-9872.

28. Moritz C and Haughton V. Functional MR imaging: paradigms for clinical preoperative mapping. *Magn Reson Imaging Clin N Am* 2003; 11: 529-542.

29. Silva AC, Williams DS, Korestsky AP. Evidence for the exchange of arterial spin-labeled water with tissue water in rat brain from diffusion-sensitized measurements of perfusion. *Magn Reson Med* 1997; 38; 232-237.

30. Schwarzbauer C, Morrissey SP, Haase A. Quantitative magnetic resonance imaging of perfusion using magnetic labeling of water protons pins within the detection slice. *Magn Reson Med* 1996; 35: 540-546.

31. Detre JA, Zhang W, Roberts DA, Silva AC, Williams DS, Grandis DJ, Koretsky AP, Leigh JS. Tissue specific perfusion imaging using arterial spin labeling. *NMR in Biomedicine* 1994; 7: 75-82.

32. Golay X, Hendrikse J, Lim TC. Perfusion imaging using arterial spin labeling. *Top Mag Reson Imaging* 2004; 15(1): 10-27.

33. Ramani R, Qiu M, Constable RT. Sevoflurane 0.25 MAC preferentially affects higher order association areas: a functional magnetic resonance imaging study in volunteers. *Anesth Analg* 2007; 105: 648-655.

34. Qiu M, Ramani R, Swetye M, Rajeevan N, Constable RT. Anesthetic effects on regional CBF, BOLD, and the coupling between task-induced changes in CBF and BOLD: an fMRI study in normal human subjects. *Magnetic Resonance in Medicine* 2008; 60: 987-996.

35. Jespersen SN and Ostergaard L. The roles of cerebral blood flow, capillary transit time heterogeneity, and oxygen tension in brain oxygenation and metabolism. *Journal of Cerebral Blood Flow & Metabolism* 2011; 1-14 [E-pub ahead of print]

36. Roy CS and Sherrington CS. On the regulation of the blood-supply of the brain. *J Physiol* 1890; 11: 85-108, 158.7-158.17.

37. Chernik DA, Gillings D, Laine H, Hendler J, Silver JM, Davidson AB, Schwan EM, Siegel JL. Validity and reliability of the observer's assessment of alertness/sedation

scale: study with intravenous midazolam. *J Clin Psychopharmacol* 1990; 10: 244-251.

38. Clouzeau B, Bui HN, Vargas F, Grenouillet-Delacre M, Guilhon E, Gruson D, Hilbert G. Target-controlled infusion of propofol for sedation in patients with non-invasive ventilation failure due to low tolerance: a preliminary study. *Intensive Care Med* 2010; 36: 1675-1680.

39. Luh WM, Wong EC, Bandettini PA, Hyde JS. QUIPSS II with thin-slice TI1 periodic saturation: a method for improving accuracy of quantitative perfusion imaging using pulsed arterial spin labeling. *Magn Reson Med* 1999; 41(6): 1246-1254.

40. Aguirre GK, Detre JA, Zarahn E, Alsop DC. Experimental design and the relative sensitivity of BOLD and perfusion fMRI. *Neuroimage* 2002; 15(3): 488-500.

41. Wong EC, Buxton RB, Frank LR. Implementation of quantitative perfusion imaging techniques for functional brain mapping using pulsed arterial spin labeling. *NMR Biomed* 1997; 10(4-5): 237-249.

42. Wang J, Aguirre GK, Kimberg DY, Roc AC, Li L, Detre JA. Arterial spin labeling perfusion fMRI with very low task frequency. *Magn Reson Med* 2003; 49(5):796-802.

43. Papademetris X, Jackowski AP, Schultz RT, Staib LH, Duncan JS. Integrated intensity and point-feature nonrigid registration. *Medical Image Computing and Computer-Assisted Intervention - Miccai* 2004, Pt 1, *Proceedings* 2004; 3216: 763-770.

44. Masamoto K, Kim T, Fukuda M, Wang P, Kim SG. Relationship between neural, vascular, and BOLD signals is isoflurane-anesthetized rat somatosensory cortex. *Cereb Cortex* 2007; 17: 942-950.

45. Oppenheimer SM, Gelb A, Girvin JP, Hachinski VC. Cardiovascular effects of human insular cortex stimulation. *Neurology* 1992; 42: 1727-1732.

46. Veselis RA, Reinsel RA, Beattle BJ, Mawlawi OR, Feshchenko VA, DiResta GR, Larson SM, Blasberg RG. Midazolam changes cerebral blood flow in discrete brain regions. *Anesthesiology* 1997; 87: 1106-1117.

47. Gray H. 1918. *Anatomy of the human body (Gray's anatomy), 20th edition.* Philadelphia: Lea and Febiger.

48. Leung HC, Gore JC, Goldman-Rakic PS. Sustained mnemonic response in the human middle frontal gyrus during on-line storage of spatial memoranda. *Journal of Cognitive Neuroscience* 2002; 14(4): 659-671.

49. Goldberg II, Harel M, Malach R. When the brain loses its self: prefrontal inactivation during sensorimotor processing. *Neuron* 2006; 50(2): 329-339.

50. Fecteau S, Pascual-Leone A, Zald DH, Liguori P, Theoret H, Boggio PS, Freni F. Activation of prefrontal cortex by transcranial direct current stimulation reduces appetite for risk during ambiguous decision making. *J Neurosci* 2007; 27(23): 6212-6218.

51. Grewe T, Bornkessel I, Zysset S, Wiese R, von Cramon DY, Shlesewsky M. The emergence of the unmarked: a new perspective on the language-specific function of Broca's area. *Hum Brain Mapp* 2005; 26(3): 178-190.

52. Veselis RA, Reinsel RA, Feshchenko VA, Wronski M. The comparative amnestic effects of midazolam, Propofol, thiopental, and fentanyl at equisedative concentrations. *Anesthesiology* 1997; 87: 749-764.

53. Veselis RA, Reinsel RA, Feshchenko VA, Dnistrian AM. A neuroanatomical construct for the amnesic effects of Propofol. *Anesthesiology* 2002; 97: 329-337.

54. Radua J, Phillips ML, Russel T, Lawrence N, Marshall N, Kalidindi S, El-Hage W, McDonald C, Giampietro V, Brammer MJ, David AS, Surguladze SA. Neural response to specific components of fearful faces in healthy schizophrenic adults. *NeuroImage* 2010; 49(1): 939-946.

55. Cavanna AE. The precuneus and consciousness. *CNS Spectr* 2007; 12(7): 545-552.

56. Hofle N, Paus T, Reutens D, Fiset P, Gotman J, Evans AC, Jones BE. Covariation of regional cerebral blood flow with delta and spindle activity during slow wave sleep in humans. *J Neurosci* 1997; 17: 4800-4808.

57. Paus T, Zatorre RJ, Hofle N, Caramanos Z, Gotman J, Petrides M, Evans AC. Time-related changes in neural systems underlying attention and arousal during the performance of an auditory vigilance task. *J Cognit Neurosci* 1997; 9: 392-408.

58. Price CJ. The anatomy of language: a review of 100 fMRI studies published in 2009. *Ann N Y Acad Sci* 2010; 1191: 62-88.

59. Heinke W, Fiebach CJ, Schwarzbauer C, Meyer M, Olthoff D, Alter K. Sequential effects of Propofol on functional brain activation induced by auditory language processing: an event-related functional magnetic resonance imaging study. *British Journal of Anaesthesia* 2004; 92(5): 641-650.

60. Liu X, Lauer KK, Ward BD, Rao S, Li SH, Hudetz AG. Propofol disrupts functional interactions between sensory and high-order processing of auditory verbal memory. *Human Brain Mapping* 2011; 1-12. [E-pub ahead of print]

61. Yurgelun-Todd DA and Ross AJ. Functional magnetic resonance imaging studies in bipolar disorder. *CNS Spectr* 2006; 11(4): 287-297.

62. Hesslink JR. The temporal lobe and limbic system. *UCSD Neuroradiology*. 29 Jan 2011. <http://spinwarp.ucsd.edu/neuroweb/Text/br-800epi.htm>.

63. Nielsen FA, Balslev D, Hansen LK. Mining the posterior cingulate: segregation between memory and pain components. *Neuroimage* 2005; 27(3): 520-532.

64. Vogt BA and Laureys S. Posterior cingulate, precuneal and retrosplenial cortices: cytology and components of the neural network correlates of consciousness. *Progress in Brain Research* 2005; 150: 205-217.

65. Bonhomme V, Fiset P, Meuret P, Backman S, Plourde G, Paus T, Bushnell MC, Evans AC. Propofol anesthesia and cerebral blood flow changes elictited by vibrotactic stimulation: a positron emission tomography study. *J Neuophysiol* 2001; 85: 1299-1308.

66. Behrendt RP. 2011. *Neuroanatomy of social behaviour: an evolutionary and psychoanalytic perspective*. London: Karnac Books Ltd 212 pp.

67. Sun X, Zhang H, Gao C, Zhang G, Xu L, Lv M, Chai W. Imaging the effects of Propofol on human cerebral glucose metabolism using positron emission tomography. *The Journal of International Medical Research* 2008; 36: 1305-1310.

68. Steriade M and Llinás RR. The functional states of the thalamus and the associated neuronal interplay. *Physiol Rev* 1988; 68(3): 649-742.

69. Xie G, Deschamps A, Backman SB, Fiset P, Chartrand D, Dagher A, Plourde G. Critical involvement of the thalamus and precuneus during restoration of consciousness with physostigmine in humans during propofol anaesthesia: a positron emission tomography study. *British Journal of Anaesthesia* 2011; 106(4): 548-557.

70. Qiu M, Ramani R, Swetye M, Constable RT. Spatial nonuniformity of the resting CBF and BOLD responses to sevoflurane: in vivo study of normal human subjects with magnetic resonance imaging. *Human Brain Mapping* 2008; 29: 1390-1399.

71. Kaufmann C, Wehrle R, Wetter TC, Holsboer F, Auer DP, Pollmächer T, Czich M. Brain activation and hypothalamic functional connectivity during human non-rapid eye movement sleep: an EEG/fMRI study. *Brain* 2006; 129: 655-667.

72. Laureys S, Owen AM, Schiff ND. Brain function in coma, vegetative state, and related disorders. *Lancet Neurol* 2004; 3: 537-546.

73. Laureys S. The neural correlate of (un)awareness: lessons from the vegetative state. *Trends Cogn Sci* 2005; 9: 556-559.

74. Jeong YB, Kim JS, Jeong SM, Park JW, Choi IC. Comparison of the effects of sevoflurane and Propofol anaesthesia on regional cerebral glucose metabolism in humans using positron emission tomography. *The Journal of International Medical Research* 2006; 34: 374-384.

75. Petersen ET, Zimine I, Ho YL, Golay X. Non-invasive measurement of perfusion: a critical review of arterial spin labeling techniques. *British Journal of Radiology* 2006; 79: 688-701.

76. Iida H, Ohata H, Iida M, Wantanabe Y, Dohi S. Isoflurane and sevoflurane induce vasodilation of cerebral vessels via ATP-sensitive K^+ channel activation. *Anesthesiology* 1998; 89: 954-960.

77. Marcar VL, Schwarz U, Martin E, Loenneker T. How depth of anesthesia influences the blood oxygen level-dependent signal from the visual cortex of children. *Am J Neuroradiol* 2006; 27: 799-805.